ELSEVIER

Microelectronic Engineering 30 (1996) 227-230

MICROELECTRONIC ENGINEERING

Modeling of in-plane distortions due to variations in absorber stress

M. Laudon[a], R. Engelstad[a], and K. Thole[a]
W. Dauksher[b], D. Resnick[b], K. Cummings[b], P. Seese[b], and W. Johnson[b]

[a]Center for X-ray Lithography, University of Wisconsin-Madison
Stoughton, WI 53589 USA

[b]Motorola, Inc., Tempe, AZ 85284 USA

The effort to achieve sub-0.25 μm X-ray lithography depends, in part, on the ability to maintain strict fabrication control leading to low distortion X-ray masks. This paper presents finite element (FE) models developed to identify sources of pattern in-plane distortions (IPD) during mask fabrication. In particular, mask fabrication processes inducing both uniform and non-uniform absorber stresses and the resulting distortions due pattern transferring through these stressed layers have been investigated.

1. INTRODUCTION

The modeling of various mask fabrication steps is essential in obtaining low final overlay errors. Specifically, mask fabrication steps such as pattern transfer through stressed layers can produce undesirable pattern in-plane distortions (IPD). Where previous work focused on membrane distortions caused by extrinsic loadings such as gravity and clamping forces [1], this paper presents verified finite element (FE) models and modeling techniques investigating pattern transfer through uniformly stressed layers. Additionally, pattern transfer through layers containing stress gradients have been found to produce much larger IPD than uniformly stressed layers [2]. Consequently verified models investigating distortions caused by pattern transfer through layers containing a linear stress gradient are presented. Thermal gradients across the substrate during plasma deposition are one possible source of these non-uniform stress distributions. An experimental thermal transient technique along with FE models have been developed to predict the steady-state temperature profiles across the membrane during plasma deposition [3]. These verified mechanical models can subsequently be used to predict final pattern distortions and optimize the related mask fabrication steps.

2. FINITE ELEMENT MODELS

Structural and heat transfer FE models of X-ray mask and membrane systems have been created using the commercially available FE code ANSYS®. Motorola style X-ray masks with 40 mm diameter membranes (see Figure 1) were used for all models and experiments discussed within this paper. The models include a Pyrex™ support ring, a silicon wafer, and either a silicon carbide or silicon nitride stressed membrane. A typical FE model is shown in Figure 2.

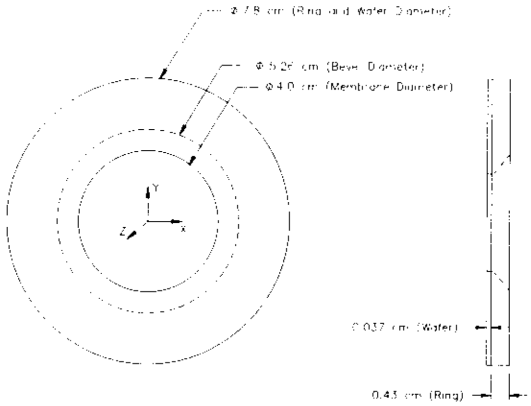

Figure 1. X-ray mask geometry (Motorola style mask) used for all models and experiments presented here.

2.1. Structural Models

All structural models employed 20-noded isoparametric solid elements for the ring and the wafer and 8-noded shell elements for the membrane material. Multi-layered stress stacks could be placed on the membrane (each layer at a different stress, thickness, and material) to simulate a realistic refractory mask. Distortions were

0167-9317/96/$15.00
SSDI 0167-9317(95)00233-2

determined due to the removal of stressed layers using an element birth/death modeling technique, thus simulating pattern transfer (etch). Reported resultant IPD are the magnitude of the maximum distortion vector within a given pattern area.

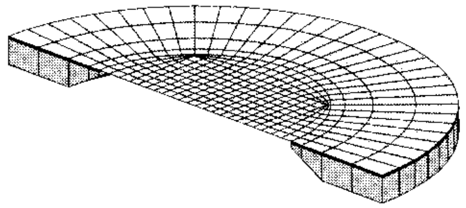

Figure 2. Typical finite element model of the Motorola style X-ray mask.

2.2. Heat Transfer Models

The FE heat transfer models use 8-noded 3-D thermal solid elements for the ring, wafer, and an aluminum cooling chuck and 4-noded 3-D thermal shell elements for the membrane. These models include convection and non-linear radiation from the membrane surface and heat conduction through the solids.

3. IPD MODEL VERIFICATION

FE models simulating changes in absorber stress were verified experimentally by fabricating X-ray masks which were patterned with full gold coverage except for a center strip. Fiducials were patterned on the membrane and the locations were measured using a Nikon 3I [4]. The gold was then heat-treated in order to increase the stress, and the corresponding distortions were measured in the fiducial pattern. A FE model (FEM) (Figure 3) with gold on a silicon carbide membrane simulated the same procedure. Figure 4 shows the finite element and experimental results for IPD versus distortion location for two different gold stress values. The FE and the experimental results are found to be in close agreement.

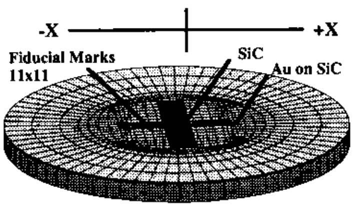

Figure 3. X-ray mask FE model with Au coverage on a SiC membrane except for the center strip.

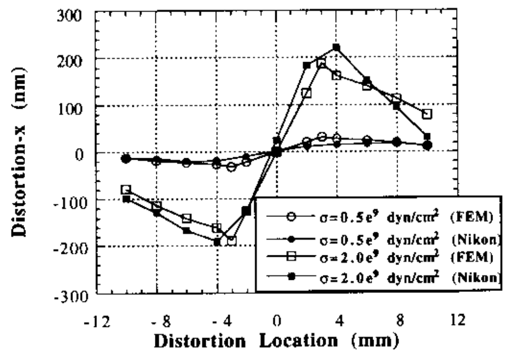

Figure 4. Experimental (Nikon) and FEM x-direction distortion due to Au stress changes versus distortion location on the x-axis.

4. UNIFORM STRESS MULTI-LAYER FEM

The verified bi-layer mechanical model was then used to investigate distortions due to pattern transfer through a multi-layered stressed stack. A FE model of a Motorola-style refractory mask was developed consisting of a Cr base, TaSiN absorber, Cr cap, and SAL601 resist deposited on a silicon nitride membrane. The stress in each layer was considered to be uniform. The model simulated the pattern transfer by incrementally removing all of the resist, Cr cap, and absorber determining the IPD caused by the removal of each layer (results shown in Table 1).

Table 1
Distortions due to layer removal.

Material	Thickness Å	Stress (dyn/cm^2)	Distortion (nm)
SAL601	3000	$2.8e^8$	3.3
Cr	200	$1.5e^{10}$	11.2
TaSiN	6000	$1.0e^8$	2.5
Cr	200	$1.5e^{10}$	
Si3N4	20000	$1.38e^9$	
(20 mm x 20 mm pattern area)		Total Distortion =	17 (radial)

Because the TaSiN is an annealable, amorphous material, the model was used to predict an absorber stress modification (before pattern transfer) to counteract the distortions caused by the stressed resist and Cr [2]. The model indicates (Figure 5) that an absorber stress of $-0.8e^9$ dyn/cm^2 would successfully eliminate the original 17 nm IPD caused by pattern transferring through the investigated layers.

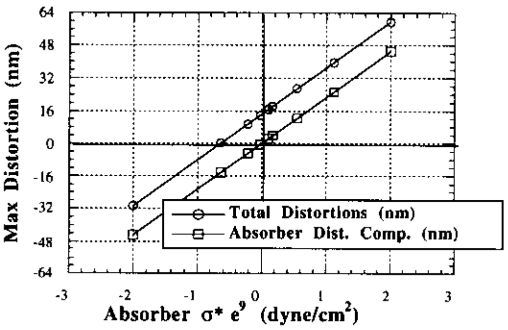

Figure 5. Maximum distortion due to pattern transfer versus absorber stress (20 mm x 20 mm pattern area). The sum of the distortions caused by pattern transfer through the resist, Cr, and absorber are shown along with the distortions caused by the absorber only.

5. LINEAR STRESS GRADIENTS

The investigations discussed above assumed that distortions were caused by pattern transfer through uniformly stressed layers. However, if a stress gradient is present in one of these layers, much larger distortions are possible [2]. Figure 6 shows a linear stress gradient present in TaSiN deposited on a 100 mm diameter wafer. The gradient is possibly due to a linear temperature gradient created during horizontal movement of the wafer in front of a plasma source. A FE model (Motorola style mask) was created with a TaSiN layer containing approximately the same stress gradient obtained experientially (Figure 7).

Figures 8 and 9 show the resulting IPD patterns due to pattern transfer through the TaSiN layer for both the experimental and FE model, respectively. Both distortion patterns exhibit the same curved shape caused by the linear stress gradient. The maximum x-direction distortion value within the 20 mm x 20 mm pattern area was found to be ±120 nm for the experimental results and ±90 nm for the FE results. There is a very close correlation between both the distortion shapes and magnitudes considering the possible differences in between the actual and modeled absorber stress gradient.

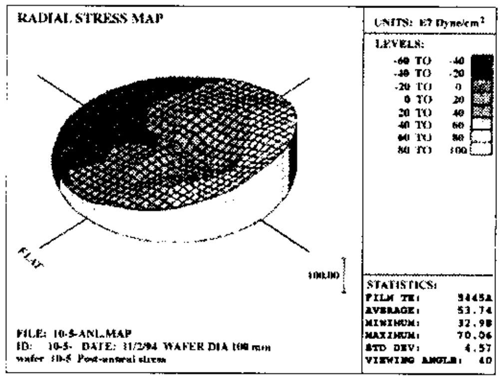

Figure 6. Linear stress gradient in TaSiN deposited upon a 100 mm diameter Si wafer. Stress levels range from $-60e^7$ dyn/cm^2 to $100e^7$ dyn/cm^2 .

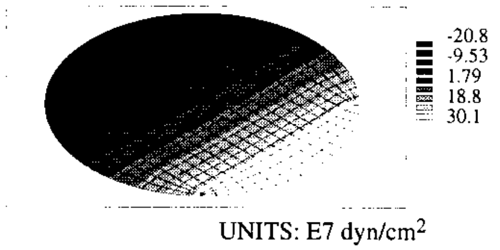

Figure 7. Modeled linear stress gradient in TaSiN over a 40 mm diameter membrane. Stress levels range from $-20e^7$ dyn/cm^2 to $30e^7$ dyn/cm^2.

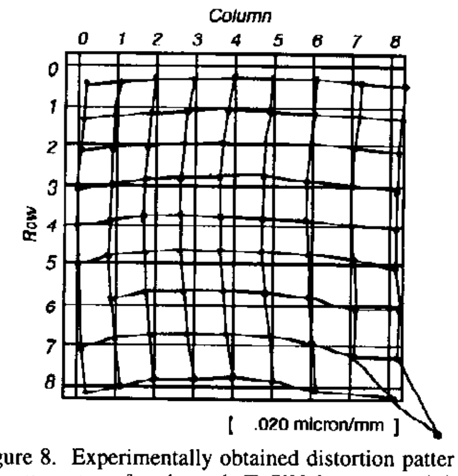

Figure 8. Experimentally obtained distortion patter due to pattern transfer through TaSiN layer containing a linear stress gradient (Maximum x-distortion ± 120 nm).

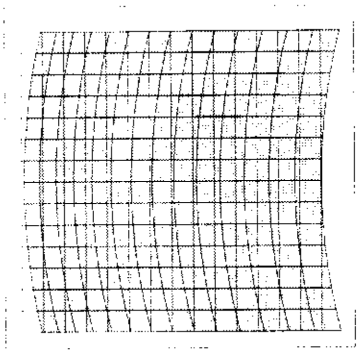

Figure 9. Finite element distortion pattern due to pattern transfer through TaSiN layer containing a linear stress gradient (maximum x-distortion ± 90 nm).

6. THERMAL GRADIENTS

The previous section focused on an absorber layer containing a linear stress gradient deposited on a wafer. Similarly, radial stress gradients can occur on a membrane due to radial temperature gradients. Due to the difficulty in measuring layer stresses on a membrane, the development of models to predict membrane temperatures during deposition are important. An experimental thermal transient technique along with FE models have been developed to predict the steady-state temperature profiles across the membrane during plasma deposition [3]. These profiles indicate that large gradients can occur depending on the membrane cooling configuration. Figure 10 shows an X-ray mask with two thermistors located on the membrane used in the verification of the FE models. Figure 11 shows the temperature profile obtained from the FE models and corresponding experimentally obtained membrane temperatures for two different cooling configurations.

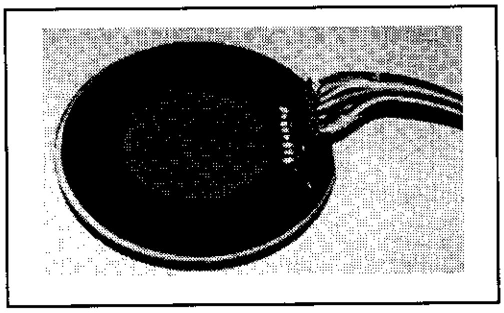

Figure 10. X-ray mask with two thermistors (center and edge) located on the membrane.

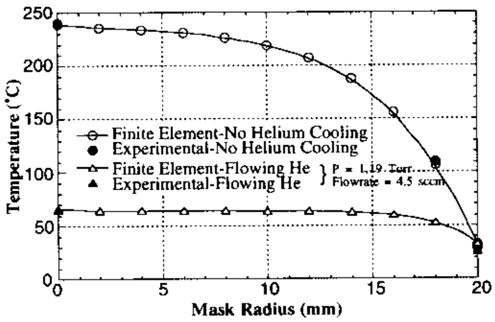

Figure 11. Finite element and experimental membrane temperature versus radius due to plasma exposure. Results for helium and no helium cooling are shown.

7. CONCLUSIONS

Results from these investigations show that the finite element models can be used as predictive tools to quantify sources of pattern distortion and to modify the individual processing steps to compensate for the incurred pattern distortions. Pattern transfer through layers containing stress gradients produce much larger distortions than uniformly stressed layers. Heat transfer FE models can be used predict and reduce thermal gradients during deposition resulting in layer stress gradients.

8. ACKNOWLEDGMENTS

This research has been supported in part by the PXLA, SRC/SEMATECH, and ARPA/NRL through the Center for X-ray Lithography at the University of Wisconsin-Madison. Additional support has been provided by the National Science Foundation and the University of Wisconsin Graduate School.

9. REFERENCES

1. D. L. Laird et al., *J. Vac. Sci. Technol. B*, Vol. 11, No. 6, (1993), pp. 2953-2957.
2. W. J. Dauksher et al., to be published in the *J. Vac. Sci. Technol. B*, (1995).
3. M. F. Laudon, et al., to be published in the *J. Vac. Sci. Technol. B*, (1995).
4. W. J. Dauksher et al., *J. Vac. Sci. Technol. B*, Vol. 12, No. 6, (1994), pp. 3990-3994.